Preprints of the 19th World Congress
The International Federation of Automatic Control
Cape Town, South Africa. August 24-29, 2014

Optimal Cell Balancing with Model-based Cascade Control by Duty Cycle Adaption

Maurice Caspar * **Sören Hohmann** *

* *Institute of Control Systems, Karlsruhe Institute of Technology, Karlsruhe Germany(e-mail: maurice.caspar@kit.edu, soeren.hohmann@kit.edu).*

Abstract: Achieving higher provided battery capacity for operation by equalizing battery cell imbalances is the goal of passive and active battery balancing systems. The idea of energy transfer between battery cells is to increase the minimal energy level of the weakest cell in a battery stack of interconnected cells. For system modeling and balancing control the drifting balancing current and changing current slope caused by the change of cell voltage has not been given attention in literature so far, as well as the formulation of balancing systems from a point of view of control theory and applying optimization algorithms to realistic scenario. Firstly, we introduce an approach based on an average mean current model for the aggregated system of battery cells and inductive balancing circuits with dependency of voltage and duty cycle. The presented non-linear model is applied to the optimization of energy distribution to minimize energy differences in a battery system in an optimal manner, which can be done for any balancing topology with the presented model. Secondly, an adaption of the duty cycle for energy transfer switching is proposed for hard realtime constraints, so that the balancing currents are maximal for the whole balancing interval. The performance of an energy-based optimization algorithm compared to a voltage-based state of the art algorithm is demonstrated by simulations as well as the proposed subordinate control approach compared without duty cycle adaption.

Keywords: energy management systems, energy storage, energy distribution, hybrid systems, modeling, cascade control, optimal control

1. INTRODUCTION

The advantages of rechargeable lithium-ion battery cells with high cycle durability, high energy and high power density compared to other battery chemistry leads to a wide field of application in automotive industry or in stationary energy storage industry. To achieve and provide the individual power and energy requirements battery cells are interconnected in series to form battery stacks with higher energy capacity and voltages. The disadvantage of lithium-ion cells is the effort of online supervision to prevent the cells from permanent damage in battery operation. For safety and ageing reasons the cells have to be kept within certain operation intervals, e.g. in between the upper and lower voltage limits, operation temperature limits and maximum charge or discharge rate limits. Therefore, a battery system requires a battery management (see Barsukov [2006], Brandl et al. [2012], Lu et al. [2013]) to guarantee safe operation conditions for all cells at all time.

1.1 Cell and State of Charge Imbalance

Part of the battery management is a cell management with charge control and battery equalization for imbalanced cells and cell states, which is necessary due to the inherent imbalance of cells. Imbalances are caused by external and internal sources. Different drain currents of integrated circuits for cell protection and supervision lead to variation of energy capacity, as well as different self discharge depending on variation of cell temperatures across the battery system (Bentley [1997]). The reason of internal sources are the imperfect results of manufacturing processes, so that even new interconnected cells in battery storages suffer from parameter variations of physical volumes, internal resistances, self discharge rates and cell capacities. Also over lifetime cells show different rates of capacity fade (cf. Baumhoefer et al. [2014]), so that a cell with initially lower capacity compared to others in a battery module can have a reduced but higher capacity compared to the others near the end of battery life.

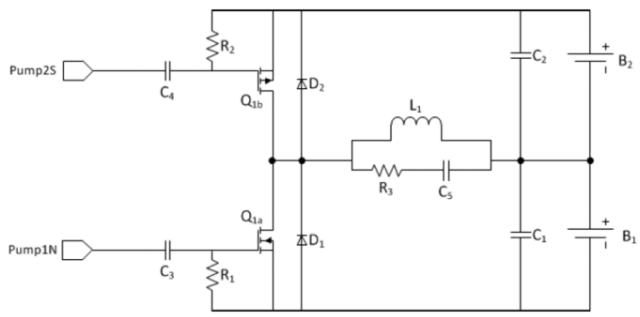

Fig. 1. Balancing circuit with energy transfer from cell to cell: Buck-Boost Converter Moran [2011]

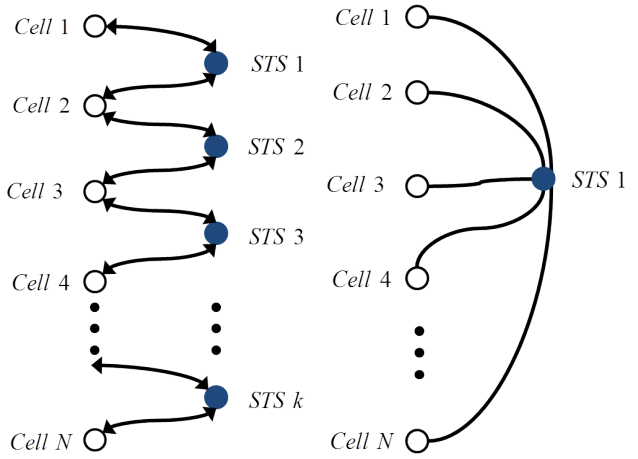

(a) Single cell to single cell (b) Stack to cell or cell to stack

Fig. 2. Examples of balancing topologies for energy transfer between battery cells

As a consequence the available energy of battery systems, consisting of a number of cells, is limited to the cell with the lowest energy capacity respectively state of charge (SOC). As a result the operation range of the whole battery system is strongly reduced due to the imbalance. Balancing circuits have been introduced in S. W. Moore [2001], Cao et al. [2008], Gallardo-Lozano et al. [2014] to avoid this limitation and to compensate the imbalance of energy capacity and SOC during operation. The energy levels in interconnected cells can be actively influenced and controlled by an energy management through these circuits.

1.2 State of the Art of Active Balancing Topologies and Structures

A various number of electric balancing systems have been developed and can be categorized into passive and active methods. Energy is removed from a cell by dissipating it as waste heat at the end of a charge process with passive dissipative balancing methods. In contrast energy can be moved with active balancing between cells via capacitors, inductors or transformers to balance the different cell energy levels. Active balancing can be used during charge and discharge operation with small energy losses due to an energy conversion efficiency less than one.

In Fig. 1 an active balancing method is shown for two interconnected cells B_1 and B_2 as an example. An energy exchange is done for instance, by charging the inductor L_1 with cell B_1 and moving the charge from inductor L_1 to cell B_2. The charge and discharge process is controlled by the two complementary pulse width modulation (PWM) signals $Pump2S$ and $Pump1N$. The circuit can be extended for N cells, which leads to a topology like in Fig. 2(a), where the white circle nodes denote battery cells and the blue circle nodes denote short-time energy storage elements.

Battery systems with a large number of cells are generally aggregated to cell modules or so called cell stacks. The modularized cells are supervised and monitored by electronic circuits, which can be controlled by a central control unit or divided in smaller decentralized slave control units which communicate with a master control unit.

Within these modules a classification of balancing systems (cf. Dong et al. [2008]) for energy transfer can be made based on the interconnection structure of cells as follows:

- Single cell to single cell method (C2C),
- Single cell to cell stack method (C2S) or
- Cell stack to single cell method (S2C).

Balancing systems also differ from each other by bidirectional (Fig. 2(a)) or unidirectional (Fig. 2(b) illustration based on Dong et al. [2008]) energy transfer possibilities. The only difference of C2S and S2C is caused by the different unidirectional transfer directions.

1.3 Control loop and State of the Art Algorithms for Active Balancing Systems

The general control loop (Fig. 3) of an active battery balancing system consists of the balancing circuit and N cells in a battery stack, which are coupled by the cell voltages $\underline{u}_{\mathrm{Cell}}$ and balancing currents $\underline{i}_{\mathrm{Bal}}$. For monitoring the cells and determining of cell states $\underline{\hat{x}}$ like SOCs and current energy levels a state observer measures the voltages $\underline{u}_{\mathrm{Cell}}$ and the external stack current i_d, which can be interpreted as a measurable disturbance of the system. The state information $\underline{\hat{x}}$ is used to calculate state setpoint or for detecting exceeding of thresholds and is forwarded to the controller. The controller is connected with a PWM generator to enable the switches with the control input $\underline{u}_{\mathrm{D}}$ of the balancing circuit for the energy transfer. The duty cycle of the PWM signal $\underline{f}$ is kept constant Moran [2011].

For balancing algorithms and controllers the state can include

- Cell voltages $u_i(t) \in [u_{\min}, u_{\max}]$ in V,
- State of charges $SOC_i(t) \in [0, 1]$ or
- Current capacities $C_i(t) \in [0, C_{\mathrm{T},i}]$ in Ah

for $i = 1, ..., N$. The State of Charge is related to the current capacity by

$$SOC_i(t) = C_i(t)/C_{\mathrm{T},i} \tag{1}$$

with the total capacity $C_{\mathrm{T},i}$ of the ith cell, which in general is different to the manufacturers nominal capacity C_{N} and changes over battery lifetime (Baumhoefer et al. [2014]). Nevertheless, an online estimation $\hat{C}_{\mathrm{T}}$ can be calculated with a model-based approach (see Plett [2011]). It has been shown in Einhorn et al. [2011], that the use of capacities as the control variable is more efficient for charging and discharging cycles than voltages or SOCs and therefore, in this contribution the preferred choice.

The complexity of control strategies depends on the interconnection structure and electric components of the circuits. Rather simple for instance is the Switched Capacitor method in Kobzev [2000], where for N cells $k = N - 1$ capacitors (topology like in Fig. 2(a)) are used for short time energy storage to shift energy. A capacitor is switched parallel to a cell to equalize to the cell voltage and then switched to an adjacent cell to equalize the two cell voltages in the long term. The switching is driven by a PWM signal with a constant duty cycle, so no complex control strategy is necessary.

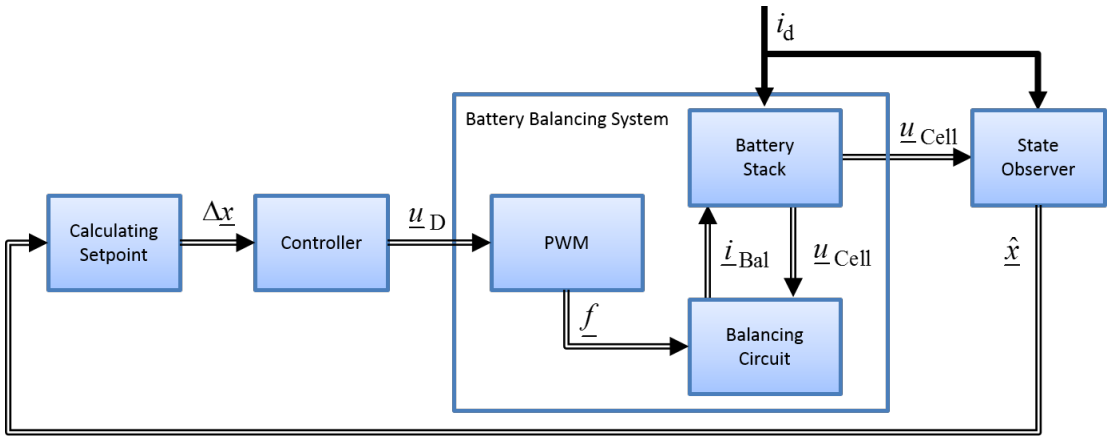

Fig. 3. Control loop of cell balancing for the battery stack systems with pulse width modulation (PWM)

As state of the art, other circuits (i.e. Fig. 1) make use of voltage information from the voltage monitoring of each cell to determine the need of energy transfer and the energy transfer direction. Differences between adjacent cells (Moran [2011]) or deviation between an average voltage in cell module compared with each individual cell (C. Bonfiglio [2009]) are calculated and used for control algorithms. These state of the art approaches of voltage based heuristic algorithms (Dong et al. [2008]) have the disadvantages of increasing complexity by increasing number of battery cells and modules, inefficiency caused by unnecessary energy transfers and imbalanced cell energies with balanced cell voltages at the end of balancing time. An improvement is the use of expert knowledge systems (Zheng et al. [2014a]), i.e. fuzzy control (Zheng et al. [2014b]), which compares the individual cell energy capacity respectively energies to determine the need of energy transfer between cells.

Recently optimal control has been introduced in Danielson et al. [2012, 2013] for storage systems. For the first time it has been mathematically proven, that in principle the problem of imbalance energies can be solved for large battery networks by energy equalization. A model-based approach is used to maximize the state of charge of large networks of battery cells. The used battery model is described by simple discrete-time integrator dynamics for the change of state of charge, where only the energy losses during the energy transfers are a function of an assumed linear relation of the cell voltage change and SOC change. The model simplifications are not suitable for cell equalization. The coupling and dependency between the battery cell and the balancing circuits, which causes time-varying balancing currents depending of the state of charges of cells, are not included in the model, so that this influence on the equalization speed of the balancing is not considered. Therefore, we propose a new model-approach with the considerations which afterwards is applied for the first time to a realistic cell balancing scenario with optimal balancing control.

1.4 Model-based Optimization of Cell Balancing

In this contribution the coupling and dependency between the battery cells and the balancing circuits are considered and part of the whole system model for a precise description of the dynamic coupling phenomena. In the following a continuous linear model of the aggregated battery stack and balancing circuit in Fig. 3 is defined, which describes the main effects of the electric behavior and the energy transfer between cells.

In a second step we use this proposed average mean current model for describing the main effects of interest to do optimal control for cell balancing. The main task of optimization is to find the optimal switching sequence to accelerate the total equalization time and minimize the energy losses by avoiding unnecessary energy transfers. We show any kind of balancing topology can be described with the model, which is used for an optimization approach to reduce long equalization times and further improvement of balancing performance. The battery stack and balancing circuit form together a hybrid system due to the switching effects of the discrete switches in the balancing subsystem (see Fig. 4(b)). But only the energy transfer integrated over time is in focus for the cell equalization, so that the behavior of the hybrid system is sufficiently described by the proposed average mean value model for the control task of balancing.

In this contribution after defining the system model in Chapter 2, it is shown in Chapter 3 how the optimization problem of determining transfer directions can be stated. Also simulation results of a comparison between a state of the art balancing algorithm and the proposed optimization approach for determining the energy transfer directions during the balancing process are presented. In Chapter 4 a subordinate control approach is introduced, which is proposed in case of hard realtime constraints. Furthermore, it is shown in Chapter 4 how the dependency of the balancing current from the individual cell voltage can be overcome, independent of the balancing algorithm, and as a result the full speed of equalization can be used for the whole cell voltage operation interval. The article ends with a conclusion in Chapter 5.

2. AVERAGE MEAN CURRENT MODEL OF BATTERY BALANCING

A lack of consideration in the optimization of the overall cell equalization is to ignore the varying balancing currents, which change over State of Charge, respectively cell voltage, because of a constant PWM signal (like in Moran

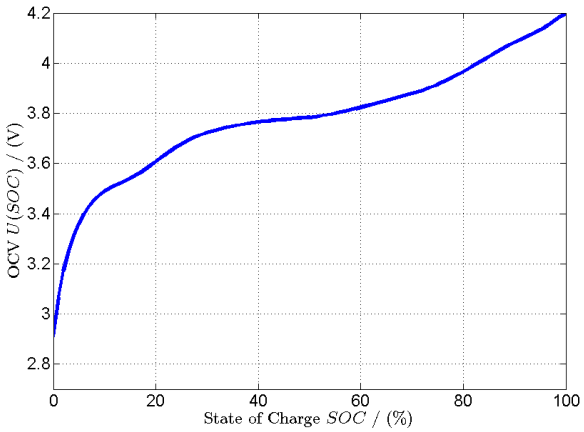

(a) Non-linear Open Circuit Voltage

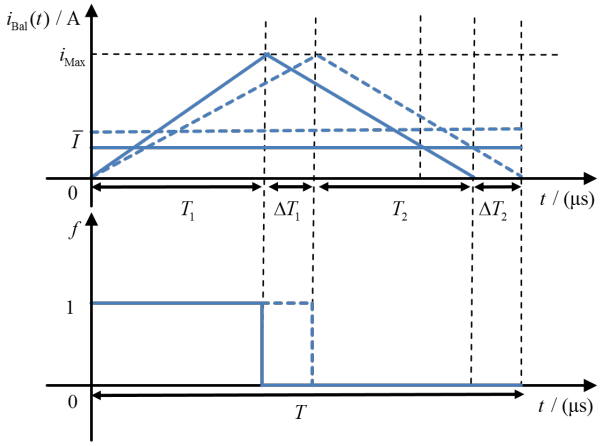

(b) Current signal and PWM trigger signal for an inductor for short-time energy storage

Fig. 4. Cell voltage dependency of SOC (a) and influence of OCV on current slope(b)

[2011]) to control the charge and discharge process between cells. Therefore, the balancing currents show a voltage-driven dependency, so that for a decreasing cell voltage the balancing current decreases as well. For instance a change from the voltage level 4.2 V to 2.7 V, leads to a decrease of current by 35 %.

In operation the balancing current purely depends on the choice of electric component parameters for short time energy storage, the duty cycle T_1/T of the switching with $T_1 \leq T/2$ and the cell voltage $u_{\mathrm{output}}(t)$. Various model approaches are used (see He et al. [2011]) to describe the electrical behavior of single cells, for instance the Thévenin model or the dual polarization model. The number of dynamic voltage elements $u_{\mathrm{RC}_i}(t)$ varies with the chosen model, but the cell voltage

$$u_{\mathrm{output}}(t) = u_{\mathrm{R}}(t) + u_{\mathrm{RC}_1}(t) + u_{\mathrm{RC}_2}(t) + U_{\mathrm{OCV}}(t) \quad (2)$$

of these models is mainly determined by the Open Circuit Voltage $U_{\mathrm{OCV}}(t)$, which has a dependency on state of charge $SOC(t)$ respectively cell energy $C(t)$.

2.1 Relation between Mean Current and Voltage Change

The control loop and optimization time is in the time domain of seconds or hours due to the capacity of cells in Ah. The short time energy storage elements like in Fig. 1 can only store a small amount of energy compared to the cell capacity for a time period of μs, and because of that the charge and discharge are repeated thousands of times per second. For the equalization the slow change of energy differences is in focus and therefore, an optimization of complete cell equalization in the time domain of μs is not appropriate and too time-consuming. It has been shown in M. Preindl [2013] that capacitors for energy transfers are slower compared to inductor and transformers balancing circuits, and therefore in the following not in focus, but the modeling approach can be applied to capacitor circuits in a similar manner.

In the following, we consider the Open Circuit Voltage (OCV) (Fig. 4(a)) for the output voltage of a single cell. Voltage drops on internal resistance and R-C elements are neglected, because of the small balancing current and fast current dynamics which leads to $u_{\mathrm{R}}, u_{\mathrm{RC}} \ll U_{\mathrm{OCV}}$. The OCV shows a non-linear dependence of SOC, which especially influences the current slope

$$\frac{\mathrm{d}i_{\mathrm{Bal}}}{\mathrm{d}t} = \frac{U_{\mathrm{OCV}}(t)}{L} \quad (3)$$

for inductor balancing circuits with the constant inductance value L. At the beginning of a duty cycle of a PWM the inductor in Fig. 1 is parallel to the first cell. The current slope of the inductor in Fig. 4(b) depends on the voltage $U_{\mathrm{OCV},1}$ until the PWM signal value changes to zero at time $t > T_1$, so that the energy in the inductor is moved to the second cell with a slope depending on $U_{\mathrm{OCV},2}$.

The mean value of the balancing current for an energy transfer from cell i to cell $i+1$ is described by

$$\bar{I}_{\mathrm{Bal},i}(t) = \frac{1}{T}\frac{U_{\mathrm{OCV},i}(t)}{L}T_1^2, \quad (4)$$

where a change of voltage $U_{\mathrm{OCV}}(t)$ leads to a change of the mean current $\bar{I}_{\mathrm{Bal},i}(t)$ for a constant time T. The voltage driven change of the mean current in (4) is depicted in Fig. 5. The depicted black area is the voltage interval, where change of SOC has the smallest impact on the change of cell voltage (see Fig. 4(a)).

2.2 Model of Aggregated Systems of Battery Stack and Balancing Circuit

The previous determined relation of current and voltage can now be applied to a battery stack, where each cell i is allocated to state $x_i(t)$. The dynamics of the system are given by

$$\dot{\underline{x}}(t) = \underline{A}\,\underline{x}(t) + \underline{B}\,(\underline{U}_{\mathrm{OCV}}, \underline{f}\,)\underline{u}_{\mathrm{D}}(t) \quad (5)$$

$$\underline{y}(t) = \underline{U}_{\mathrm{OCV}}(\underline{x}(t)) \quad (6)$$

with the system matrix consisting of zero matrix $\underline{A} = \underline{O}$, the state $\underline{x} \in [0, C_{\mathrm{T},i}]^N$ for all cells with $i = 1, ..., N$ and input $\underline{u}_{\mathrm{D}} \in \{0,1\}^M = \mathcal{U}$. The input dimension M is a function h of the number k of energy storages in a balancing circuit with $M = h(2k)$, when each energy short-time storage element has bidirectional energy transfer directions. In the output equation the OCV for each cell

is denoted by $\underline{U}_{\mathrm{OCV}} \in [u_{\min}, u_{\max}]^N$. The input matrix $\underline{B}$ is given by

$$\underline{B} = \underline{L} \cdot \underline{Q}_{\overline{\mathrm{I}}}(\underline{U}_{\mathrm{OCV}}, \underline{f}) \tag{7}$$

with the matrix $\underline{L} \in \mathbb{R}^{N \times M}$ and the mean current matrix

$$\underline{Q}_{\overline{\mathrm{I}}}(\underline{U}_{\mathrm{OCV}}, \underline{f}) = \mathrm{diag}(\overline{I}_{\mathrm{Bal,1}}, ..., \overline{I}_{\mathrm{Bal,N}}) \tag{8}$$

with $\underline{Q}_{\overline{\mathrm{I}}} \in \mathbb{R}_+^{M \times M}$ and $\underline{f} \in \mathbb{R}_+^M$. The model structure and interaction of the controller with the battery system by the system input $\underline{u}_{\mathrm{D}}$ is depicted in Fig. 6. In contrast to the proposed topology matrix in M. Preindl [2013], the matrix $\underline{L}$ also includes the energy losses caused by the energy transfers between cells. Furthermore, the model is now nonlinear.

3. BALANCING OPTIMIZATION ALGORITHM WITH CONSTANT PWM

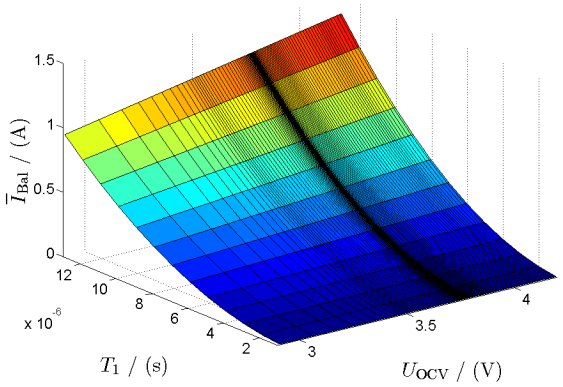

Fig. 5. Current change: Influence of OCV U_{OCV} and switching time T_1 on mean balancing current $\overline{I}_{\mathrm{Bal}}$

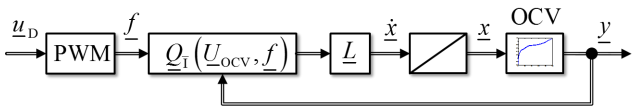

Fig. 6. Mean current model of battery cell stack and balancing circuit

3.1 Control Goal and Set Point

The goal of active balancing is to increase the battery energy usage during battery operation. For in series connected cells the overall capacity of a battery stack

$$C_{\mathrm{Stack}}(t) = \min\{C_i(t)\}_{i=1,...,N} \tag{9}$$

is determined by the cell with the lowest capacity. The control goal is to increase the stack capacity

$$\max_{\underline{u}_{\mathrm{D}}(t) \in \mathcal{U}} C_{\mathrm{Stack}}(t) = \max_{\underline{u}_{\mathrm{D}}(t) \in \mathcal{U}} \min\{C_i(t) + \int_0^t I_{\mathrm{Bal},i}\, \mathrm{d}\tau\} \tag{10}$$

for $i = 1, ..., N$ by balance the imbalanced energy levels $C_i(t)$ while charging and discharging operation.

The average capacity of a whole battery stack arises from the sum of each cell capacity which yields to

$$x_{\mathrm{set,i}}(t) = \overline{C}_{\mathrm{Stack}}(t) = \frac{1}{N} \sum_{i=1}^{N} C_i(t) \tag{11}$$

for the set point $x_{\mathrm{set},i}$ of the control task. The set point changes over time due to the losses of the energy transfers, so that $x_{\mathrm{set},i}(t_1) \geq x_{\mathrm{set},i}(t_2)$ for $t_1 < t_2$. The balancing process can be stopped, when the battery cells have reached an equilibrium state for which

$$\lim_{t \to \infty} \left(\min\{C_i(t) + \int_0^t I_{\mathrm{Bal},i}\, \mathrm{d}\tau\} - \overline{C}_{\mathrm{Stack}}(t) \right) = 0 \tag{12}$$

is fulfilled.

3.2 Optimal Cell Balancing

A transformation of the continuous model with (5) and (6) to a discrete model opens up new possibilities for interpreting the input $\underline{u}_{\mathrm{D}}(k)$ and for the optimization of the balancing process. The system input $\underline{u}_{\mathrm{D}}(t)$ has been defined in the restricted discrete domain $\underline{u}_{\mathrm{D}} \in \{0,1\}^M$ and can be extended to $\underline{u}_{\mathrm{D}} \in [0,1]^M$ as an adjustable, arbitrary input between the limits with the time discretization T_{Dis}. An input $u_{\mathrm{D},i}$ less than one means that between two time instances k and $k+1$ the PWM signal is not applied the whole time interval. As a result the balancing current can be controlled between the limits $[0, \overline{I}_{\max}(k)]$ for the optimization between time k and $k+1$.

In Chapter 3.1 the control goal of active balancing has been discussed, where the maximizing of the interconnected cell is in focus. Therefore, the objective of the balancing optimization problem is to minimize the energy differences of cells $\Delta x_i(t) = C_i(t) - \overline{C}_{\mathrm{Stack}}(t)\ \forall i$ and to minimize the power loss for energy transfer subject to operation and cell interconnection constraints. The problem can be formulated as follows

$$\min_{\underline{u}(k)} (c_1 \left\| \underline{x}(k) - \overline{\underline{x}}(k) \right\|_1^2 + c_2 \left\| \underline{u}(k) \right\|_1^2] + c_3 \cdot k_f) \tag{13}$$

$$\begin{aligned} &s.t. \\ &\underline{x}(k+1) = \underline{x}(k) + T_{\mathrm{Dis}} \cdot \underline{B}\, \underline{u}(k) \\ &\underline{x}(0) = \underline{x}_0 \\ &\underline{x}(k_f) = \overline{\underline{x}} = \frac{1}{N} \sum_{i=1}^{N} |x_i(0)| \\ &\underline{u}(k) \in [0,1]^{\mathrm{M}} \end{aligned}$$

with coefficients $c_i > 0$ and under the constraint that parallel bidirectional energy transfers between the two states x_i to x_j are not allowed at the same time. The instant of time k_f denotes the end of the optimization, when $C_i(k = k_f) = x_{\mathrm{set},i}(k = k_f)\ \forall i$.

The optimization problem in (13) can be solved by using a standard dynamic optimization algorithm. For the following simulations direct collocation has been chosen, because of the good approximation of the integrator dynamics of the system in (5) and (6) by this method.

3.3 Simulation Parameters, Results and Discussion

In the following the performance of a state of the art voltage-based balancing algorithm is compared with an energy-based optimization algorithm, which solves the optimization problem stated in (13) for the control input $\underline{u}_{\mathrm{D}}$ for a balancing process. A cell equalization is simulated for 8 battery cells with cell to cell balancing circuits like the Buck-Boost Converter in Fig. 1 extended for 8 cells.

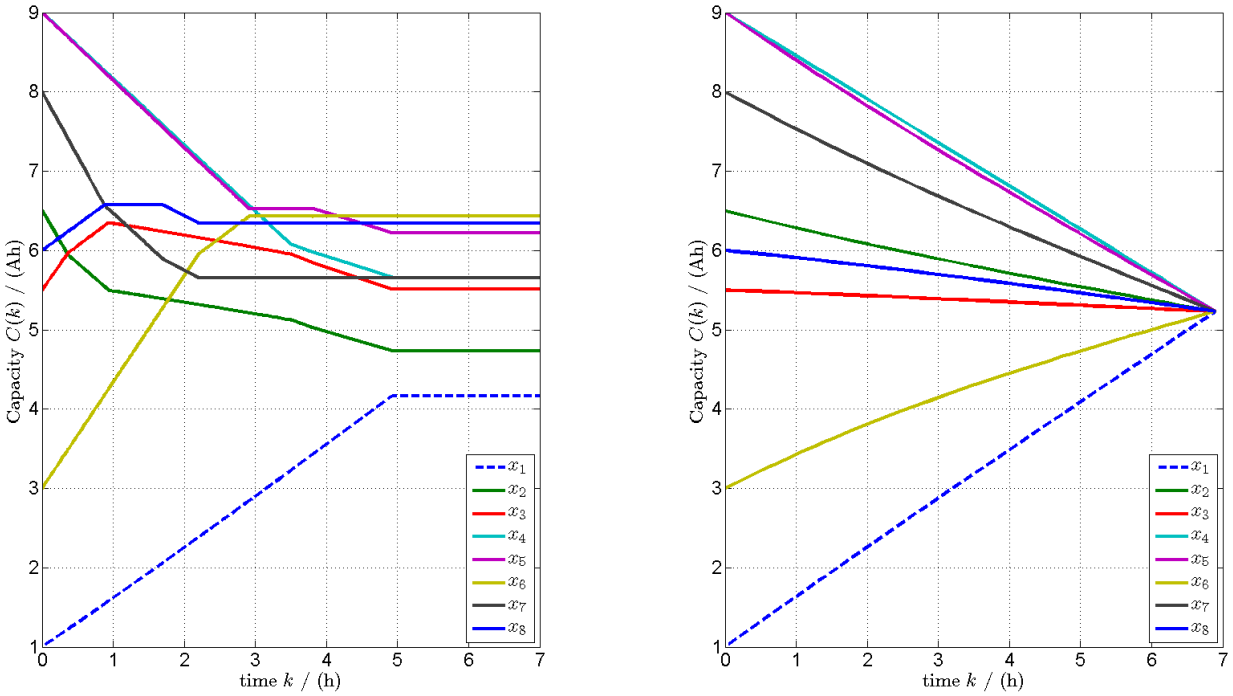

(a) Voltage based state of the art approach

(b) Model and energy based optimization approach

Fig. 7. Simulation results of balancing: Change of energy levels of each cell state $C_i(k)$ over time t

Thus, the balancing system model from (5) is defined for the simulations by the matrix

$$\underline{L} = \begin{pmatrix} -1 & \mu & 0 & 0 & 0 & 0 & 0 & 0 & 0 & 0 & 0 & 0 & 0 & 0 \\ \mu & -1 & -1 & \mu & 0 & 0 & 0 & 0 & 0 & 0 & 0 & 0 & 0 & 0 \\ 0 & 0 & \mu & -1 & -1 & \mu & 0 & 0 & 0 & 0 & 0 & 0 & 0 & 0 \\ 0 & 0 & 0 & 0 & \mu & -1 & -1 & \mu & 0 & 0 & 0 & 0 & 0 & 0 \\ 0 & 0 & 0 & 0 & 0 & 0 & \mu & -1 & -1 & \mu & 0 & 0 & 0 & 0 \\ 0 & 0 & 0 & 0 & 0 & 0 & 0 & 0 & \mu & -1 & -1 & \mu & 0 & 0 \\ 0 & 0 & 0 & 0 & 0 & 0 & 0 & 0 & 0 & 0 & \mu & -1 & -1 & \mu \\ 0 & 0 & 0 & 0 & 0 & 0 & 0 & 0 & 0 & 0 & 0 & \mu & -1 & -1 \end{pmatrix}$$

with the circuit-depending efficiency constant μ for energy transfers and the mean current matrix

$$\underline{Q}_{\overline{\mathrm{I}}} = \begin{pmatrix} \overline{I}_1 & 0 & 0 & 0 & 0 & 0 & \cdots & & 0 \\ 0 & \overline{I}_2 & 0 & 0 & 0 & 0 & \cdots & & 0 \\ 0 & 0 & \overline{I}_2 & 0 & 0 & 0 & \cdots & & 0 \\ 0 & 0 & 0 & \overline{I}_3 & 0 & 0 & \cdots & & 0 \\ 0 & 0 & 0 & 0 & \overline{I}_3 & 0 & \cdots & & 0 \\ \vdots & \vdots & \vdots & \vdots & \ddots & \ddots & \ddots & & 0 \\ & & & & & 0 & \overline{I}_{\mathrm{N}-1} & 0 & 0 \\ & & & & & 0 & 0 & \overline{I}_{\mathrm{N}-1} & 0 \\ 0 & 0 & 0 & 0 & 0 & 0 & 0 & 0 & \overline{I}_{\mathrm{N}} \end{pmatrix}$$

with the balancing current $\overline{I}_i = \overline{I}_{\mathrm{Bal},i}(\underline{U}_{\mathrm{OCV}}(t), \underline{f}(t))$. The OCV curve shown in Fig. 4(b) is used for the output equation in (6). Further simulation parameters, initial conditions and initial states are given in Table A.1.

For the simulation the state of the art algorithm compares the actual voltages $u_{\mathrm{OCV},i}(t)$ of two adjacent cells i and j with $i \neq j$ beginning from the top of the battery stack to bottom. Energy from the cell with higher voltage is moved to the cell with lower voltage, when the voltage difference exceeds the limit of $c_{\mathrm{V,limit}} = 10$ mV. The results of the state of the art approach are shown in Fig. 7(a) for the change of cell energy levels. At the beginning energy from cell state x_4 is moved through cell state x_3 and state x_2 to cell state x_1. Parallel cell state x_5 loads cell state x_6 and cell state x_7 loads cell state x_8 until cell state x_7 is leveled with x_8, so that the energy transfer changes to the opposite direction to load state x_8 together with state x_5 till the end of balancing at time $k_f = 4.93$ h.

The optimization problem due to (13) has been solved by using a dynamic optimization algorithm (direct collocation). The used optimization parameters are given in Table A.1. The results of the optimization approach are shown in Fig. 7(b) for the change of cell energy levels. All cell states x_i show no alternating of charging and discharging till the end of balancing at time $k_f = 6.89$ h, and therefore, no energy is wasted by unnecessary energy transfers.

After the initial time $k = 0$ with the average stack capacity 6.00 Ah the stack capacity of the state of the art approach $C_{\mathrm{Stack}}(k_{f,1})$, indicated with the black line in Fig. 8, is similar at the beginning in comparison to the capacity of the optimization approach shown indicated with the blue line. For $k > 4.93$ h the state of the art approach leads to no further capacity improvement in contrast to the optimization algorithm. The optimization approach leads to a balanced battery stack 117.6 min after the state of the art approach stopped, which still suffers of energy imbalances. Additionally, the final stack capacity $C_{\mathrm{Stack}}(k_{f,2})$ is 17.6 % higher in relation to the initial stack

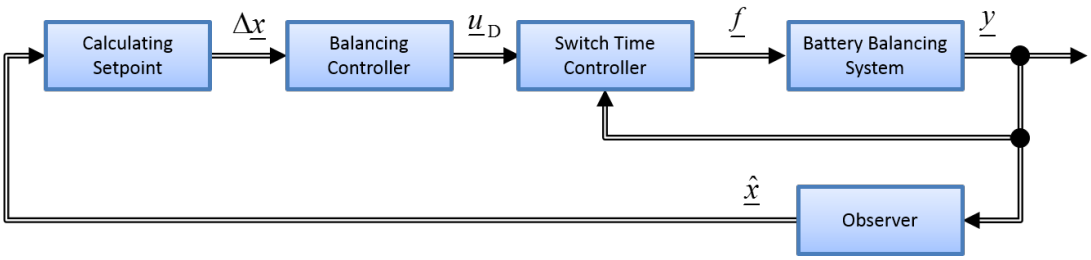

Fig. 9. Control loop of cell balancing and battery stack with cascade control

capacity at time $k = 0$, due to the more efficient energy transfer with 5.23 Ah in contrast to 4.17 Ah with the state of the art approach. For the optimal approach the stack capacity $C_{\mathrm{Stack}}(k_{f,2})$ is equal to the average capacity of the stack at the end of the balancing process in contrast to the state of the art approach.

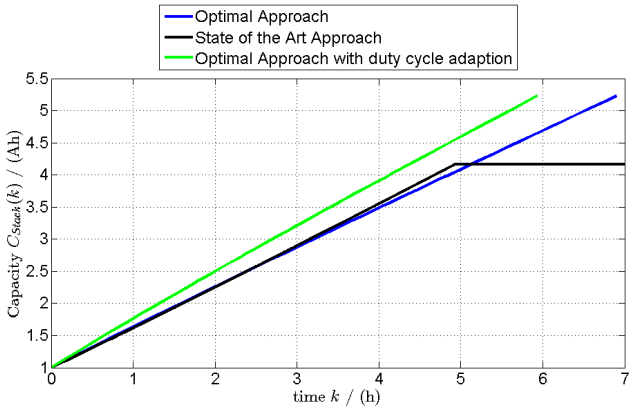

Fig. 8. Effective cell module capacity $C_{\mathrm{Stack}}(k)$

4. OPTIMIZATION WITH PWM ADAPTION

4.1 Varying Balancing Currents

Maximizing the balancing current over the full range of state of charge leads to an acceleration of the equalization process. In the following is shown how the dependency of the balancing current from the individual cell voltage can be overcome and the full speed of equalization can be used for the whole cell voltage operation interval. Instead of a constant PWM signal for the switching mechanism, a adaption of the duty cycle is proposed (Fig. 9) to maximize the balancing current for any state of charge.

4.2 Duty Cycle Adaption

The decrease of voltage U_{OCV} can be compensated by an increase of the switch time T_1 to keep the balancing current $\overline{I}_{\mathrm{Bal}}$ constant on the maximal level. The switching time can be adapted with ΔT_1 for the balancing current

$$\overline{I}_{\mathrm{const}} = \overline{I}_{\mathrm{Bal}}(t) = \frac{1}{2T}\frac{1}{L}(U + \Delta U)(T_1 + \Delta T_1)^2, \quad (14)$$

for all t during charging and discharging operation, when a voltage drift ΔU occurs and yields to

$$\Delta T_1 = \sqrt{2\,T\,L\frac{\overline{I}_{\mathrm{const}}}{U + \Delta U}} - T_1 \quad (15)$$

to counteract the change of current slope $\mathrm{d}i_{\mathrm{Bal}}/\mathrm{d}t$ by compensating the change of voltage ΔU. The adaption of T_1 can occur through a subordinate control loop (Fig. 9) by adding the measured cell voltage $\underline{U}(t)$ as an extra input signal to the PWM block in Fig. 6 for calculating the required time ΔT_1. As a consequence the input matrix $\underline{Q}_{\overline{\mathrm{I}}}(\underline{U}_{\mathrm{OCV}}, \underline{f}) = \mathrm{diag}(\overline{I}_{\max}, ..., \overline{I}_{\max})$ consists of entries with the balancing current of maximal $\overline{I}_{\max}$ level for $\forall t$. As a result the state space system is described by

$$\dot{\underline{x}}(t) = \underline{B}\ \underline{u}_{\mathrm{D}}(t) \quad (16)$$
$$\underline{y}(t) = \underline{U}_{\mathrm{OCV}}(\underline{x}(t)) \quad (17)$$

with the constant input matrix $\underline{B}$, which only includes the maximum balancing currents $\overline{I}_{\max,i}\ \forall i$.

4.3 Simulation Results with PWM Adaption

The results of the approach with and without duty cycle adaption are shown in Fig. 8, the optimal approach from the previous Chapter without the duty cycle adaption is depicted in blue and the optimal approach with duty cycle adaption in green. Due to the duty cycle adaption the current slope difference can be clearly recognized and leads to a balancing acceleration of $k_f = 5.93$ h compared to $k_f = 6.89$ h. In comparison with the state of the art approach, which is indicated with the black line in Fig. 8, the duty cycle adaption leads to a higher stack capacity at all times as well.

An investigation of the frequency distribution and harmonics by analyzing the Fast Fourier Transformation of the PWM signal has shown, that the duty cycle adaption leads to negligible small changes of the frequency distribution of PWM signal due to the small changes of the switch times.

5. CONCLUSION

A model with consideration of the battery cell and balancing circuit dependencies has been presented, which has been used for improving battery balancing performances by a model-based optimal balancing algorithm to find the optimal input switching sequence. It has been shown that a real time optimization approach can reduce the energy losses by reducing the total amount of moved energy between cells during the balancing process as well as the model-based balancing approach increases the available capacity by 17.6 % in contrast to a suboptimal state of the art balancing approach. The insight of the model dependencies has given rise to an approach for duty cycle adaption, which has been introduced to keep balancing currents on the maximal possible level at all times, which

can be even applied to non model-based balancing. The compensation of the current voltage dependency by the proposed duty cycle adaption was validated by simulations and a performance time speed up by 16 % has been shown for an example. As a result of the optimal utilization of the balancing circuits the minimal capacity in a battery cell stack was increased in comparison to constant duty cycle operation at all times.

REFERENCES

D. Barsukov, Y. ; Freeman. Better battery management through digital control. *Power Electronics Technology*, 1:30–35, 2006.

T. Baumhoefer, M. Bruehl, S. Rothgang, and D. U. Sauer. Production caused variation in capacity aging trend and correlation to initial cell performance. *Journal of Power Sources*, 247(0):332 – 338, 2014. ISSN 0378-7753.

W. F. Bentley. Cell balancing considerations for lithium-ion battery systems. In *Battery Conference on Applications and Advances, 1997., Twelfth Annual*, pages 223–226, 1997.

M. Brandl, H. Gall, M. Wenger, V. Lorentz, M. Giegerich, F. Baronti, G. Fantechi, L. Fanucci, R. Roncella, R. Saletti, S. Saponara, A. Thaler, M. Cifrain, and W. Prochazka. Batteries and battery management systems for electric vehicles. In *Design, Automation Test in Europe Conference Exhibition (DATE), 2012*, pages 971 –976, 2012.

W. Roessler C. Bonfiglio. A cost optimized battery management system with active cell balancing for lithium ion battery stacks. In *Vehicle Power and Propulsion Conference, 2009. VPPC '09. IEEE*, pages 304 –309, sept. 2009.

J. Cao, N. Schofield, and A. Emadi. Battery balancing methods: A comprehensive review. In *Vehicle Power and Propulsion Conference, 2008. VPPC '08. IEEE*, pages 1 –6, 2008.

C. Danielson, F. Borrelli, D. Oliver, D. Anderson, M. Kuang, and T. Phillips. Balancing of battery networks via constrained optimal control. In *American Control Conference (ACC), 2012*, pages 4293 –4298, 2012.

C. Danielson, F. Borrelli, D. Oliver, D. Anderson, and T. Phillips. Constrained flow control in storage networks: Capacity maximization and balancing. *Automatica*, 49(9):2612 – 2621, 2013.

G. X. Dong, Y. S. Yan, Y. Wei, and H. Jun. Analysis on equalization circuit topology and system architecture for series-connected ultra-capacitor. In *Vehicle Power and Propulsion Conference, 2008. VPPC '08. IEEE*, pages 1–5, 2008.

M. Einhorn, W. Roessler, and J. Fleig. Improved performance of serially connected li-ion batteries with active cell balancing in electric vehicles. *Vehicular Technology, IEEE Transactions on*, 60(6):2448 –2457, july 2011.

J. Gallardo-Lozano, E. Romero-Cadaval, M. I. Milanes-Montero, and M. A. Guerrero-Martinez. Battery equalization active methods. *Journal of Power Sources*, 246 (0):934 – 949, 2014.

H. He, R. Xiong, and J. Fan. Evaluation of lithium-ion battery equivalent circuit models for state of charge estimation by an experimental approach. *Energies*, 4 (4):582–598, 2011.

G.A. Kobzev. Switched-capacitor systems for battery equalization. In *Modern Techniques and Technology, 2000. MTT 2000. Proceedings of the VI International Scientific and Practical Conference of Students, Postgraduates and Young Scientists*, pages 57–59, 2000.

L. Lu, X. Han, J. Li, J. Hua, and M. Ouyang. A review on the key issues for lithium-ion battery management in electric vehicles. *Journal of Power Sources*, 226:272–288, 2013.

F. Borrelli M. Preindl, C. Danielson. Performance evaluation of battery balancing hardware. In *European Control Conference 2013*, 2013.

J. Moran. Powerpump balancing. Technical report, Texas Instrument, October 2011. SLUA524B.

G. L. Plett. Recursive approximate weighted total least squares estimation of battery cell total capacity. *Journal of Power Sources*, 196(4):2319 – 2331, 2011.

P. J. Schneider S. W. Moore. A review of cell equalization methods for lithium ion and lithium polymer battery systems. In *SAE 2001 World Congress, Detroit, MI,*, 2001.

Y. Zheng, M. Ouyang, L. Lu, J. Li, X. Han, and L. Xu. On-line equalization for lithium-ion battery packs based on charging cell voltages: Part 1. equalization based on remaining charging capacity estimation. *Journal of Power Sources*, 247(0):676 – 686, 2014a.

Y. Zheng, M. Ouyang, L. Lu, J. Li, X. Han, and L. Xu. On-line equalization for lithium-ion battery packs based on charging cell voltages: Part 2. fuzzy logic equalization. *Journal of Power Sources*, 247(0):460 – 466, 2014b.

Appendix A. MODEL PARAMETERS FOR BALANCING SIMULATION

Table A.1. Simulation parameters

Description	Parameter	value	unit
Cell state 1	$x_1(0)$	1	Ah
Cell state 2	$x_2(0)$	6.5	Ah
Cell state 3	$x_3(0)$	5.5	Ah
Cell state 4	$x_4(0)$	9	Ah
Cell state 5	$x_5(0)$	9	Ah
Cell state 6	$x_6(0)$	3	Ah
Cell state 7	$x_7(0)$	8	Ah
Cell state 8	$x_8(0)$	6	Ah
Total capacity cell 1	$C_{\mathrm{T},1}$	37	Ah
Total capacity cell 2	$C_{\mathrm{T},2}$	39	Ah
Total capacity cell 3	$C_{\mathrm{T},3}$	42	Ah
Total capacity cell 4	$C_{\mathrm{T},4}$	40	Ah
Total capacity cell 5	$C_{\mathrm{T},5}$	41	Ah
Total capacity cell 6	$C_{\mathrm{T},6}$	43	Ah
Total capacity cell 7	$C_{\mathrm{T},7}$	38	Ah
Total capacity cell 8	$C_{\mathrm{T},8}$	40	Ah
Power loss constant	μ	0.8	-
Max balancing current	$\overline{I}_{\max}$	1	A
Charge time	T_1	$11, 11$	μs
Interval time	T	$27, 77$	μs
Inductance	L	9.4	μH
Optimization coefficient	c_1	1	-
Optimization coefficient	c_2	100	-
Optimization coefficient	c_3	1000	-